Ultramicroscopy 137 (2014) 48–54

Contents lists available at ScienceDirect

Ultramicroscopy

journal homepage: www.elsevier.com/locate/ultramic

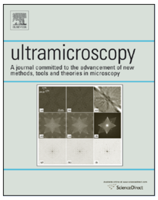

Height drift correction in non-raster atomic force microscopy

Travis R. Meyer [a], Dominik Ziegler [b], Christoph Brune [c], Alex Chen [d], Rodrigo Farnham [e], Nen Huynh [e], Jen-Mei Chang [e], Andrea L. Bertozzi [a,1], Paul D. Ashby [b,*]

[a] Department of Mathematics, University of California Los Angeles, Los Angeles, CA 90095, USA
[b] Molecular Foundry, Lawrence Berkeley National Laboratory, Berkeley, CA 94720, USA
[c] Institute for Computational and Applied Mathematics, University of Münster, Germany
[d] Statistical and Applied Mathematical Sciences Institute, Research Triangle Park, NC 27709, USA
[e] Department of Mathematics and Statistics, California State University Long Beach, Long Beach, CA 90840, USA

ARTICLE INFO

Article history:
Received 21 June 2013
Received in revised form
14 October 2013
Accepted 25 October 2013
Available online 4 November 2013

Keywords:
Atomic force microscopy
Self-intersecting scan
Drift correction
Non-raster scan

ABSTRACT

We propose a novel method to detect and correct drift in non-raster scanning probe microscopy. In conventional raster scanning drift is usually corrected by subtracting a fitted polynomial from each scan line, but sample tilt or large topographic features can result in severe artifacts. Our method uses self-intersecting scan paths to distinguish drift from topographic features. Observing the height differences when passing the same position at different times enables the reconstruction of a continuous function of drift. We show that a small number of self-intersections is adequate for automatic and reliable drift correction. Additionally, we introduce a fitness function which provides a quantitative measure of drift correctability for any arbitrary scan shape.

1. Introduction

Atomic Force Microscopy (AFM) measures the interaction force between a sharp tip and sample to acquire high resolution images by serially scanning a sample area while recording these minute interactions often at sub-nanometer resolution [1–4]. The fact that AFM achieves high resolution imaging over a large variety of sample types and environments makes it one of the most frequently used characterization tools in nanoscience. As AFM mechanically detects sub-nanometer size features, its accuracy is easily compromised by drift. Drift mainly originates from thermal fluctuations resulting in the slow expansion and contraction of instrument parts. Traditionally, in raster scanning height drift, or z-drift, is corrected using flattening. Flattening is performed by removing a low order polynomial fit from each scan line. This rudimentary technique often results in artifacts where sample features become partially removed or tilted. Extracting accurate topographic data, therefore, often requires the user to choose an appropriate combination of different flattening techniques.

Part of the rationale for a raster pattern is that the data samples align with a regular grid, making the data ideal for visualizing in a pixelated image. For each data point raster scanning requires the probe tip to be at a specific location at a given time. But non-linearities such as hysteresis and creep associated with the multidomain properties of high sensitivity piezoelectric materials make this a difficult engineering task [5–8]. We have shown that these problems can be overcome with Sensor Inpainting techniques [9] which use advanced inpainting algorithms [10–15] to generate accurate images based on position sensor data, see Appendix A. The technique, furthermore, frees scanning probe microscopy from the paradigm of raster scanning so that data recorded along any arbitrary path can be used to generate an image.

This enables the use of sinusoidal scan patterns that require less bandwidth and are better suited to drive high inertia nanopositioners [16–19]. Fig. 1 shows an Archimedean spiral as a typical non-raster scan path. For legibility we show a scan path with only five loops for the inward (solid line) and outward scans (dashed line). Raster scanning typically only uses either trace or retrace data for generating an image, but in Sensor Inpainting 100% of the data can be displayed and at least a two-fold increase in temporal or spatial resolution is achieved. For high temporal resolution inward and outward scans can be used separately, and for higher lateral resolution a single image can be generated using the data collected on the inward and outward scan together. As

---

[*] Corresponding author. Tel.: +1 510 486 7081.
E-mail addresses: bertozzi@math.ucla.edu (A.L. Bertozzi), pdashby@lbl.gov (P.D. Ashby).
[1] Tel.: +1 310 825 4340.

http://dx.doi.org/10.1016/j.ultramic.2013.10.014
0304-3991

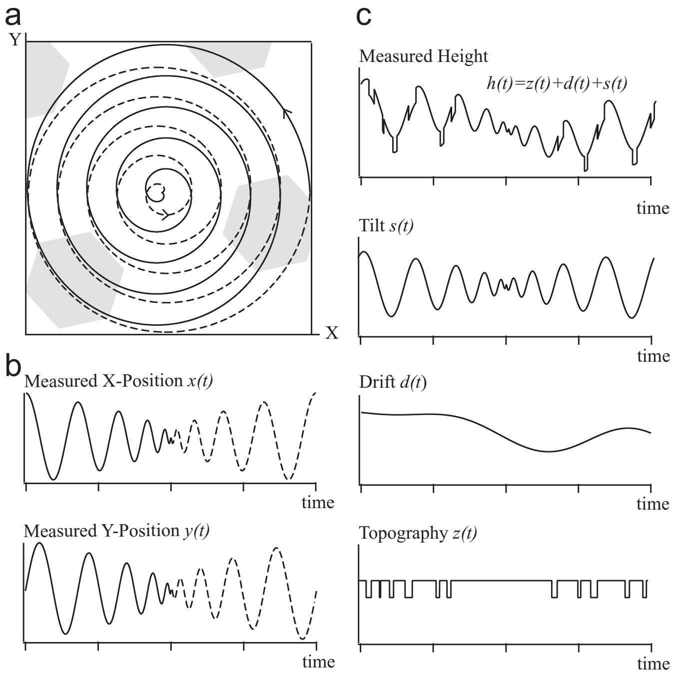

Fig. 1. (a) Illustration of a five loop Archimedean spiral showing inward (solid line) and outward (dashed line) scan paths. The gray hexagons illustrate recessed topographic features. (b) Measured X and Y positions versus time. (c) The measured height $h(t)$ along the scan pass comprises effects from the tilt $s(t)$, drift $d(t)$ as well as the real topography $z(t)$ which we aim to recover as accurately as possible to generate a clean topographic image.

shown in Fig. 1(c) the recorded height $h(t)$ typically contains contributions from the tilt of the sample $s(t)$ and drift of the instrument $d(t)$. In the presence of drift, the same point in space may have different measured heights because of temporal separation. It is therefore extremely important to have reliable methods to detect and correct drift in non-raster scan AFM. Using Sensor Inpainting the tip is not required to follow a linear motion. As a consequence, sample tilt does not necessarily result in a linear feature in the recorded height time trace. Fig. 2 shows our attempt to generalize the naïve fit-and-flatten approach to non-raster scan paths. Fig. 2(a) shows a time trace recorded using a non-raster scan pattern over a calibration grating with 8 nm deep features. A continuous piecewise linear fit is overlaid. The corrected height signal is shown in the bottom panel. It is clear that the linear fitting distorts many of the features. Without distinguishing drift from tilt any fitting algorithm will potentially distort the measured topography and result in loss of reliability. Furthermore, for a non-raster scan it is not obvious how to best choose the length of the linear segments for line flattening. In Fig. 2(b) we show an Archimedean spiral scan on evaporated gold; the individual grains are visible but rings in the raw image resulted from drift. Piecewise linear fitting can flatten these artifacts if the appropriate number of segments is chosen ($N=300$). The technique suffers from the same problems as flattening techniques in raster scan AFM where height information can easily be altered by the flattening and having too many segments results in a loss of topographic information ($N=3000$). The requirement to find the right flattening parameters makes the technique unreliable. In Section 2 we introduce drift detection using self-intersecting scan paths. Our new method requires no human interaction and is significantly more accurate since it detects and corrects drift independent of sample topography or tilt, unlike flattening which convolutes drift and topography. In Section 3 we discuss the performance the self-intersection method, and finally in Section 4 we present a summary and conclusion.

2. Drift correction using self-intersecting scans

2.1. *Self-intersecting scan patterns*

Our method for measuring and correcting drift is based on measuring the height at a known position but different times. This requires the scan pattern to self-intersect, but as Sensor Inpainting [9] can generate an image from any arbitrary scan path, we are free to use any suitable path. Fig. 1(a) shows the most commonly used non-raster scan pattern: the double Archimedian spiral (DAS). Note that inverting the Y drive signal for the outward spiral (dashed line) maintains a counter-clockwise motion and leads to a continuous path with no abrupt changes in scan direction and, more importantly, it introduces two self-intersections per loop. Fig. 3(a) shows such a spiral scan with 25 loops. The location of the self-intersections are indicated by red dots, all of which lie on a line. Measuring the height of a given position twice with only small temporal separation does not give a good measure of drift, and since thermal drift occurs on large time scales, scan paths with intersections of large temporal separation contain information better suited for the detection and correction of drift. In the modulated double Archimedean spiral (MDAS) shown in Fig. 3 (b) the number of self-intersections and their temporal and spatial distribution is increased by perturbing one spatial coordinate with a sine wave of period equal to the scan time and amplitude of one-tenth of the scan size. Fig. 3(c) shows a Spirograph, another type of sinusoidal scan pattern which generates many more self-intersections. In Section 2.4 we will introduce a fitness function which provides a quantitative measure for drift correctability for each of these scan forms. However, its description requires the introduction of the least squares difference method first.

2.2. *Finding intersections*

The first step in using the differences method for drift compensation is to find the self-intersections of the curve that represents the scan path. For a well-defined curve in continuous space, intersections are equally well-defined. When the curve is represented by discrete samples, however, the problem becomes somewhat more complex and ill-defined. As the AFM's position sensor gives quantized information at a finite sampling rate, the intersection detection algorithm can easily generate false intersections, throwing off the differences fitting energy. To combat this issue, we convolve each of the position sensor signals with a Gaussian smoothing function with a standard deviation on the same order as the smallest resolved distance by the sensors. One solution is to compose the N discrete samples $\{\vec{x}_i\}_{i=1}^{N}$ of the curve into $N-1$ connected line segments joining adjacent samples described by

$$X_i = \{(1-t)\vec{x}_i + t\vec{x}_{i+1} | t \in (0,1]\}.$$

Then the line segments can be checked against each other for intersections in $O(N^2)$ time by checking all possible intersections pair-wise. For a more detailed description of the algorithm see Appendix B.

2.3. *Least squares differences algorithm*

Error in the height measurement due to z-drift is locally approximately linear and can be modeled as a smooth function with small second derivative. This assumption together with the existence of path self-intersections motivate our approach. Let $\vec{x}(t)$ be a vector containing $x(t)$ and $y(t)$ that describes the scan path i.e. position of the AFM probe on the sample. Using accurate sensors to measure these positions we can assume minimal position errors. As introduced in Fig. 1 the height signal measured